Color superconducting matter in a magnetic field

Kenji Fukushima[1,*] and Harmen J. Warringa[2,†]

[1]*RIKEN BNL Research Center, Brookhaven National Laboratory, Upton, NY 11973, USA*
[2]*Department of Physics, Bldg. 510A, Brookhaven National Laboratory, Upton, NY 11973, USA*

(Dated: July 25, 2007)

We investigate the effect of a magnetic field on cold dense three-flavor quark matter using an effective model with four-Fermi interactions with electric and color neutrality taken into account. The gap parameters Δ_1, Δ_2, and Δ_3 representing respectively the predominant pairing between down and strange (d-s) quarks, strange and up (s-u) quarks, and up and down (u-d) quarks, show the de Haas-van Alphen effect, i.e. oscillatory behavior as a function of the modified magnetic field $\tilde{B}$ that can penetrate the color superconducting medium. Without applying electric and color neutrality we find $\Delta_2 \simeq \Delta_3 \gg \Delta_1$ for $2\tilde{e}\tilde{B} > \mu_{\rm q}^2$, where $\tilde{e}$ is the modified electromagnetic coupling constant and $\mu_{\rm q}$ is one third of the baryon chemical potential. Because the average Fermi surface for each pairing is affected by taking into account neutrality, the gap structure changes drastically in this case; we find $\Delta_1 \gg \Delta_2 \simeq \Delta_3$ for $2\tilde{e}\tilde{B} > \mu_{\rm q}^2$. We point out that the magnetic fields as strong as presumably existing inside magnetars might induce significant deviations from the gap structure $\Delta_1 \simeq \Delta_2 \simeq \Delta_3$ at zero magnetic field.

PACS numbers: 12.38.Aw, 12.38.-t, 24.85.+p, 26.60.+c

arXiv:0707.3785v1 [hep-ph] 25 Jul 2007

By analyzing Quantum Chromodynamics (QCD) it has been established that at zero temperature and high enough baryon densities color superconducting (CSC) matter should be formed [1]. Unfortunately no experimental evidence for color superconductivity is yet available. In CSC matter Cooper pairs of quarks are created due to an attractive interaction between quarks on opposite sides of the Fermi surface. The (almost) sole place where one might be able to find color superconductivity in nature would be the central part of neutron stars. To this aim one has to clarify the properties of CSC matter under the physical conditions maintained inside neutron stars [2, 3].

The neutron star density is at most $\rho \sim 10\rho_0$ in the core, where ρ_0 is the normal nuclear density $\sim 0.17\,\text{nucleon/fm}^3$. This density roughly corresponds to a quark chemical potential (i.e. one third of the baryon chemical potential) $\mu_{\rm q} \sim 500$ MeV as deduced from $\rho \sim 3\mu_{\rm q}^3/\pi^2$. At this intermediate density one cannot neglect the role of the strange quark mass $M_s = 100 \sim 200$ MeV. The strange quark mass induces a "pressure" to tear the Cooper pairs apart, i.e., a Fermi surface mismatch of size $M_s^2/2\mu_{\rm q}$ between u/d quarks and s quarks will be formed. The pairing pattern is quite complicated in the density region where $M_s^2/2\mu_{\rm q}$ is comparable to the gap energy Δ which are both of order tens MeV around the region of our interest where $\mu_{\rm q} \sim 500$ MeV.

The Fermi surface mismatch is further caused by the requirement of neutrality which is broken by $M_s \neq 0$ in three-flavor quark matter. The system should be electric neutral to avoid divergent field energies faster than the volume, otherwise the system is not stable thermodynamically. Regarding color neutrality the constraint is more stringent, that is, the whole system must be a color-singlet. To consider the phase structure, however, it is adequate to impose global color neutrality as well as global electric neutrality. In the effective model we will use in this Letter this can be achieved by introducing the electric and color chemical potentials, μ_e, μ_3, and μ_8 corresponding the the *negative* electric charge matrix $Q_e = -Q = \text{diag}(-\frac{2}{3}, \frac{1}{3}, \frac{1}{3})$ in flavor space and two diagonal color charge matrices $T_3 = \text{diag}(\frac{1}{2}, -\frac{1}{2}, 0)$ and $T_8 = \text{diag}(\frac{1}{3}, \frac{1}{3}, -\frac{2}{3})$ in color space [4]. These chemical potentials mimic gauge field dynamics.

In neutron stars another source for the "pressure" on Cooper pairs is a magnetic field. In regular neutron stars the magnetic field strength on the surface is of order $B = 10^9 \sim 10^{12}$ G and it reaches values as large as $B \sim 10^{15}$ G (in which case $eB = 1 \sim 10\ \text{MeV}^2$) in a special kind of neutron star called magnetar [5]). Actually the virial theorem [6] enables us to deduce $B \lesssim 10^{18}$ G in the interior of the neutron star. In compact stars that are self-bound rather than gravitationally bound, the maximum magnetic field could be even larger such that $eB \approx \mu_{\rm q}^2$. Clearly, the effect of these magnetic fields are not to be neglected at all as compared to Δ and $M_s^2/2\mu_{\rm q}$.

Much work has been done to investigate the effect of the magnetic field on nuclear matter (see Ref. [3] and references therein) and also some on normal quark matter [7, 8] but only limited results [9, 10, 11, 12] are available on CSC matter in a penetrating magnetic field.

In particular in Ref. [10] the analytical solution of the gap equation is found only in the limit of a strong magnetic field without taking account of the neutrality conditions. The new material we shall elucidate in this Letter is twofold; first, we solve the gap equations numerically in order to get the gap parameters for any value of magnetic field within the framework of the Nambu–Jona-Lasinio (NJL) model. This model correctly describes qualitative

features of high-density QCD [1, 13]. Next, we impose the electric and color neutrality conditions on the system which changes the qualitative behavior of the gap parameters significantly from the non-neutral case.

We assume only the predominant pairing in the color anti-symmetric channel;

$$\langle\bar{\psi}_{i\alpha}\gamma_5 C\bar{\psi}^T_{j\beta}\rangle \sim \epsilon_{1\alpha\beta}\epsilon_{1ij}\Delta_1+\epsilon_{2\alpha\beta}\epsilon_{2ij}\Delta_2+\epsilon_{3\alpha\beta}\epsilon_{3ij}\Delta_3\,, \quad (1)$$

where α and β run from 1 to 3 in color space (r,g,b) and i and j run from 1 to 3 in flavor space (u,d,s). The gap parameters Δ_1, Δ_2, and Δ_3 represent the ds-pairing, su-pairing, and ud-pairing, respectively.

This gap pattern breaks the electromagnetic U(1) symmetry. As a result the photon becomes massive, so that a pure electromagnetic field cannot penetrate CSC matter. However, the pairing pattern is still invariant under $\mathrm{U}(1)_{\tilde{Q}}$ transformations, where $\tilde{Q} = \mathbf{1}_{\rm color}\otimes Q - Q\otimes\mathbf{1}_{\rm flavor}$. The corresponding rotated electromagnetic field is $\tilde{A}_\mu = A_\mu\cos\theta - G^Q_\mu\sin\theta$, which is a combination of the electromagnetic field A_μ and a component of the gluonic field G^Q_μ. The rotated photon stays massless, hence a rotated magnetic field $\tilde{B}$ can penetrate CSC matter [9]. The coupling constant for $\tilde{A}$ is $\tilde{e} = e\cos\theta$ where e and g are the electromagnetic and QCD coupling constant. Here the mixing angle θ may depend on the gap structure [9, 14]. In the convention that the gauge fields are defined with generators normalized as $\mathrm{tr}[t_a t_b] = 2\delta_{ab}$, one finds $\cos\theta = g/(\frac{1}{3}e^2+g^2)^{1/2}$ for color-flavor locked (CFL) matter ($\Delta_1 \approx \Delta_2 \approx \Delta_3$). For the phases with only Δ_2 or Δ_3 nonzero (i.e. 2SCsu or 2SC phase) one has $\cos\theta = g/(\frac{1}{12}e^2+g^2)^{1/2}$. Interestingly enough, we find that the mixing angle in the phase with only Δ_1 nonzero (i.e. 2SCds phase) is the same as that in the CFL phase [15].

By careful consideration of the boundary layer between CSC matter and normal quark matter one can derive a relation between the magnitude of the applied external magnetic field $B_{\rm ext}$ outside and the rotated magnetic field $\tilde{B}$ inside CSC matter. For sharp boundaries (boundary smaller than screening length) a small part of the flux is expelled and one has $\tilde{B} \approx B_{\rm ext}\cos\theta$, while for smooth boundaries $\tilde{B} \approx B_{\rm ext}$ hence no flux is expelled at all. [9]. Since $g \gg e$ in the region we are interested in, $\cos\theta \approx 1$ which implies that the magnitudes of the magnetic fields outside and inside the CSC core are approximately equal, that is, we will implicitly assume $\tilde{e}\tilde{B} \approx eB_{\rm ext}$ in our discussions.

While the quark Cooper pairs are neutral with respect to the $\tilde{Q}$ charge, some of the individual quarks which form a pair are, however, charged under the $\tilde{B}$ field. In particular, the three flavors and three colors result in nine different quarks from which four are $\tilde{Q}$ charged. We summarize in the following table the quark species, $\tilde{Q}$, and the gap parameters involved in the pairing;

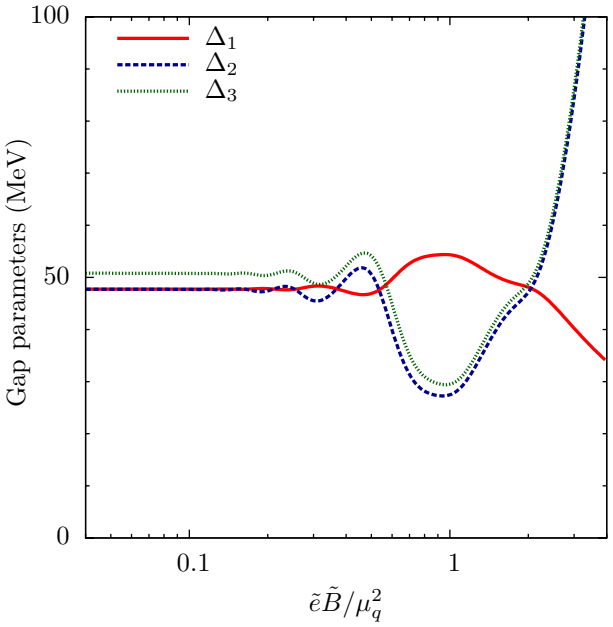


FIG. 1: Gap parameters as a function of $\tilde{e}\tilde{B}/\mu_{\rm q}^2$ for $\mu_{\rm q} = 500$ MeV without neutrality.

pairing	ru	gd	bs	bd	gs	rs	bu	gu	rd
$\tilde{Q}$	0	0	0	0	0	+1	−1	−1	+1
gap	Δ_1	Δ_2	Δ_3	Δ_1		Δ_2		Δ_3	

For the charged sectors a constant magnetic field results in the Landau quantization of the energy dispersion relation. For instance, the rs-bu sector of the Nambu-Gor'kov propagator contains sixteen dispersion relations as a function of $p^2 = p_x^2 + p_y^2 + p_z^2$. Once we turn on a constant $\tilde{B}$ in the z-direction, rotational symmetry is broken and the dispersion relations are modified by the following replacement,

$$p^2 \to p_B^2 = 2|\tilde{e}\tilde{B}|(n+\tfrac{1}{2}) \pm |\tilde{e}\tilde{B}| + p_z^2\,, \quad (2)$$

where $n = 0, 2, 3\ldots$ with $\pm|\tilde{e}\tilde{B}|$ depending on the spin and $\tilde{Q}$ charge. Then, in order to write down the thermodynamic potential Ω of the NJL model, we can utilize the conventional expression (see e.g. Ref. [16] including full account of $M_s \neq 0$) with the prescription (2) for the rs-bu and gu-rd sectors. The associated momentum integration is modified as follows

$$\int \frac{dp_x dp_y}{(2\pi)^2} \to \frac{|\tilde{e}\tilde{B}|}{2\pi}\sum_{n=0}^{\infty}\,. \quad (3)$$

We will present the prove of this simple replacement in a separate paper [15].

We first solve three gap equations without neutrality taken into account,

$$\frac{\partial\Omega}{\partial\Delta_1} = \frac{\partial\Omega}{\partial\Delta_2} = \frac{\partial\Omega}{\partial\Delta_3} = 0 \quad (4)$$

at $\mu_e = \mu_3 = \mu_8 = 0$ to check consistency with Ref. [10].

We show our numerical results as a function of a dimensionless parameter $\tilde{e}\tilde{B}/\mu_{\rm q}^2$ in Fig. 1 for $\mu_{\rm q} = 500$ MeV. We chose the cut-off parameter $\Lambda = 1000$ MeV and the four-Fermi coupling constant to yield $\Delta_0 = 50$ MeV for $M_s = \tilde{B} = 0$. We made sure that Λ-dependence is tiny once the coupling constant runs as a function of Λ to give a fixed value of Δ_0. To reduce the cut-off artifact, we used a smooth Fermi-Dirac-like form factor, $\frac{1}{2}\{1 - \tanh[(p_B - \Lambda)/\omega]\}$ with a choice $\omega = 0.1\Lambda$ in the momentum integration. If we adopt a smaller value of ω which results in a sharper cut-off scheme, the curves in Fig. 1 become less smooth. In particular, for $\omega \to 0$ we find tiny spikes in the gap parameters when $\Lambda^2/(2\tilde{e}\tilde{B})$ is an integer, originating from the vacuum energy contribution to the thermodynamic potential. We have checked the robustness of the smooth oscillatory shapes seen in Fig. 1 by varying the value of ω [15].

We can see that Δ_2 and Δ_3 are close to each other apart from a discrepancy by the strange quark mass which is $M_s = 100$ MeV in our calculation; the effect of M_s pushes Δ_1 and Δ_2 down to 47.7 MeV and Δ_3 up to 50.8 MeV at $\tilde{B} = 0$. The gap parameters show oscillatory behavior as long as $2\tilde{e}\tilde{B} < \mu_{\rm q}^2$ because the density of states increases every time $2\tilde{e}\tilde{B}n$ approaches $\mu_{\rm q}^2$ for some non-zero n. Thus, the oscillation ceases when the first Landau level ($n = 1$) lies above the Fermi surface, i.e. $2\tilde{e}\tilde{B} > \mu_{\rm q}^2$. In fact, it is manifest in Fig. 1. The behavior of the gap parameters is similar to the oscillation of the magnetization of a material in an external magnetic field which is known as the de Haas-van Alphen effect.

Our numerical results are qualitatively consistent with the analytical evaluation in Ref. [10] for $\tilde{e}\tilde{B} \gg \mu_{\rm q}^2$ when only the lowest Landau level (LLL) contributes to the gap equations. In that case the gap parameters Δ_2 and Δ_3 increase monotonically as a function of $\tilde{B}$. The reason for this is understood in view of the analytical expressions given by Eqs. (95) and (96) in the second paper of Ref. [10]; roughly speaking, as a result of the LLL approximation, the phase space is enlarged as $2\mu_{\rm q}^2 \to \mu_{\rm q}^2 + \tilde{e}\tilde{B}$. At the same time we see that Δ_1 decreases slightly as a function of $\tilde{B}$ because it is only indirectly sensitive to $\tilde{B}$, which is qualitatively consistent with Eq. (101) in Ref. [10].

Next we will impose three neutrality conditions,

$$\frac{\partial\Omega}{\partial\mu_e} = \frac{\partial\Omega}{\partial\mu_3} = \frac{\partial\Omega}{\partial\mu_8} = 0\,. \tag{5}$$

We have also added the contribution of a free electron and muon gas to Ω. Electrons and muons feel the magnetic field $\tilde{B}\cos\theta$ with the coupling constant e, that amounts to $e\tilde{B}\cos\theta = \tilde{e}\tilde{B}$. Once we take account of neutrality the situation drastically changes. Figure 2 shows the gap parameters with μ_e, μ_3, and μ_8 determined self-consistently for $\mu_{\rm q} = 500$ MeV. The corresponding chemical potentials are displayed in Fig. 3. It can be seen in Fig. 3

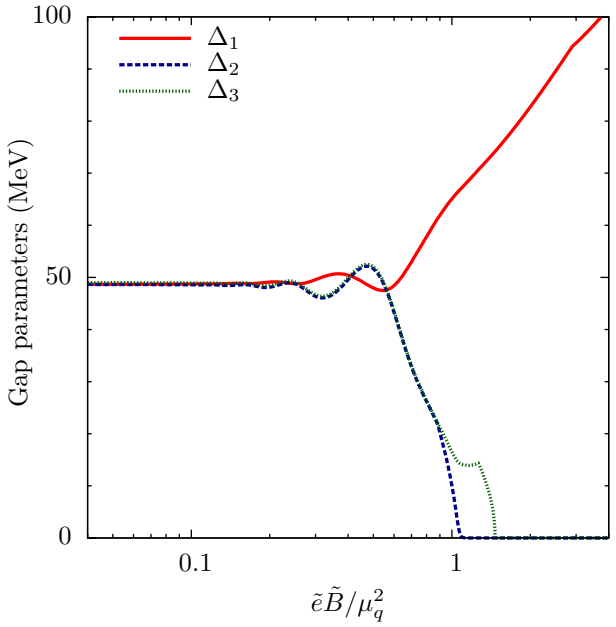


FIG. 2: Gap parameters as a function of $\tilde{e}\tilde{B}/\mu_{\rm q}^2$ with neutrality, for $\mu_{\rm q} = 500$ MeV.

that at very large $\tilde{e}\tilde{B}$, μ_e is larger than the muon mass $\simeq 106$ MeV. This indicates that in that case a significant number of muons will be present in the system.

In sharp contrast to the non-neutral case, we find that Δ_1 grows with increasing $\tilde{e}\tilde{B}$. The gap parameters Δ_2 and Δ_3 vanish smoothly at $\tilde{e}\tilde{B}/\mu_{\rm q}^2 \simeq 1.09$ and 1.47, respectively. This implies a second order transition from the CFL phase to the so-called dSC phase, followed by a transition to the so-called 2SCds phase. Note that the mixing angle θ is common in the CFL, dSC, and 2SCds phases. The behavior of Δ_1 at large $\tilde{e}\tilde{B}$ can be accounted for by μ_3 and μ_8; the Fermi surface average $\bar{\mu}_{bd\text{-}gs}$ becomes larger, for example in our calculation, from 500 MeV at $\tilde{B} = 0$ to 625 MeV at $\tilde{e}\tilde{B}/\mu_{\rm q}^2 = 4$. This results in a larger gap parameter. So the system exhibits a phase with only Δ_1 nonzero at large $\tilde{e}\tilde{B}/\mu_{\rm q}^2$. This implies two-flavor color superconducting pairing between d and s quarks, hence the name 2SCds. The possibility of the 2SCds phase as a ground state for $\tilde{e}\tilde{B}/\mu_{\rm q}^2 > 1.47$ is quite interesting, since the 2SCds phase has rarely been paid attention to in the QCD phase diagram. [See Ref. [17] for detailed analyses including the 2SCds region.]

The 2SCds phase is similar to the more familiar 2SC phase where only Δ_3 takes a finite value. The behavior of μ_3 and μ_8 in the 2SCds region might look totally different from the 2SC phase in which $\mu_3 = 0$ and $\mu_8 \ll \mu_e$. This difference, however, turns out superficial once we rearrange the color-flavor bases properly as $\mu_3' = \mu_8 - \frac{1}{2}\mu_3$ and $\mu_8' = -\frac{1}{2}\mu_3 - \mu_8 - \frac{3}{2}\mu_e$. Then, as shown by dotted curves in Fig. 3, μ_3' in the 2SCds phase is zero just like μ_3 in the 2SC phase, and μ_8' stays smaller than μ_e just like

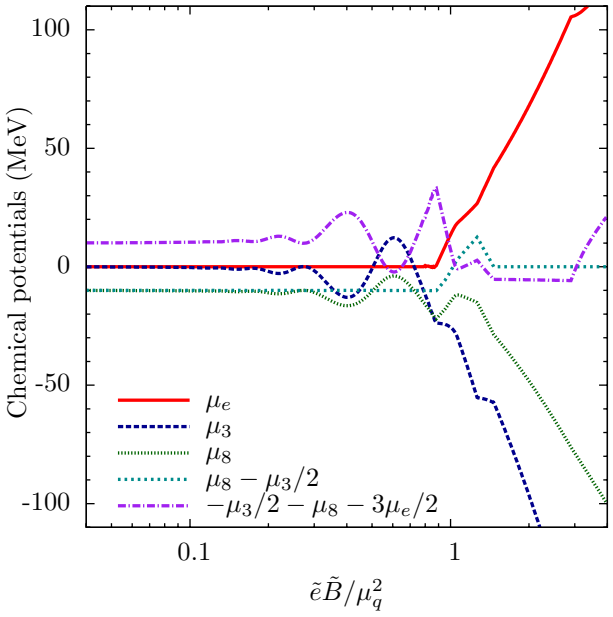


FIG. 3: Chemical potentials as a function of $\tilde{e}\tilde{B}/\mu_{\rm q}^2$, for $\mu_{\rm q} = 500$ MeV.

μ_8 in the 2SC phase. We note that μ_3' is not oscillatory at all even though μ_3 and μ_8 are. We also point out that CFL matter remains a $\tilde{Q}$-insulator, i.e. $\mu_e = 0$ [18] until $\tilde{e}\tilde{B}/\mu_{\rm q}^2 \simeq 0.88$.

In fact, there are two windows in which gapless dispersion relations with non-zero gap parameters appear; $0.88 < \tilde{e}\tilde{B}/\mu_{\rm q}^2 < 1.09$ for *rs-bu* pairing with Δ_2 and $1.25 < \tilde{e}\tilde{B}/\mu_{\rm q}^2 < 1.47$ for *gu-rd* pairing with Δ_3. The 2SCds phase for $\tilde{e}\tilde{B}/\mu_{\rm q}^2 > 1.47$ is fully gapped. Once the system enters the gapless state, Δ_2 and Δ_3 rapidly decrease to zero. Because the phase space is enlarged by large $\tilde{B}$ for $\tilde{Q}$-charged quarks and thus their density increases, the Fermi surface averages $\bar{\mu}_{rs\text{-}bu}$ and $\bar{\mu}_{gu\text{-}rd}$ should be located lower than the others to keep neutrality. It can happen with developing $\mu_3 \neq 0$ and $\mu_8 \neq 0$ which alter not only the Fermi surface averages but also the Fermi surface mismatches $\delta\mu_{rs\text{-}bu}$ and $\delta\mu_{gu\text{-}rd}$. Under the constraint of neutrality, hence, Δ_2 and Δ_3 become smaller because of the decreasing Fermi surface average with increasing $\tilde{B}$, and at the same time, the Fermi surface mismatches for Δ_2 and Δ_3 grow up with μ_3 and μ_8 induced by $\tilde{B}$, and eventually the gapless dispersion relations emerge when $\delta\mu_{rs\text{-}bu} > \Delta_2$ or $\delta\mu_{gu\text{-}rd} > \Delta_3$.

The question of whether the 2SCds phase is a real possibility of the ground state under a sufficiently strong magnetic field or not should be answered by energy comparison with normal quark matter. We have to calculate the energy density in CSC matter with $\tilde{e}\tilde{B}$ and that in normal quark matter with $eB_{\rm ext}$ to determine which is energetically favored. Unfortunately the energy density has a huge oscillation as a function of $\tilde{B}$ if $\tilde{e}\tilde{B} \simeq \Lambda^2$. This oscillation arises from the vacuum energy contributions to the thermodynamic potential. Because normal quark matter couples in another way to the magnetic field, the oscillation in the energy density of normal quark matter is different from that of CSC matter, making energy comparison at $\tilde{e}\tilde{B} \simeq \Lambda^2$ ambiguous.

We have carefully checked that the cut-off dependence is tiny in the gap equations and neutrality conditions as we mentioned, and it is natural because the momentum integration near the Fermi surface should be dominant. Therefore we could as well have taken a larger value of Λ such that the gap parameters remain to have the same value and $\tilde{e}\tilde{B}$ is much smaller than Λ^2. In this way we found that there is always an energy gain between CSC and normal quark matter, in particular it is kept to be at least 2×10^8 MeV^4 around $\tilde{e}\tilde{B}/\mu_{\rm q}^2 \sim 1$.

However the field energy it takes to expel part of the applied magnetic field from CSC matter is in the case of a sharp boundary equal to $\frac{1}{2}(B_{\rm ext}^2 - \cos^2\theta B_{\rm ext}^2) \lesssim e^2 B_{\rm ext}^2/6g^2$. The coefficient e^2/g^2 is of order 0.01, and therefore, the energy cost is of order 1×10^8 MeV^4 around $\tilde{e}\tilde{B}/\mu_{\rm q}^2 \sim 1$, which is comparable or less than the energy gain. In the case of a smooth boundary no flux is expelled at all, so then CSC matter is always favored. We might thus expect to see $\Delta_1 \gg \Delta_2 \simeq \Delta_3$ before reaching a possible transition to normal quark matter. Hence if $eB_{\rm ext} \approx \mu_{\rm q}^2$, the 2SCds phase could be a likely candidate for the ground state of matter inside magnetars.

In summary, we considered the effect of a strong magnetic field on neutral CSC quark matter. We found that the neutrality conditions significantly change the non-neutral results. We pointed out the possibility of the 2SCds phase in the interior of the magnetar.

K. F. thanks T. Kunihiro and M. Tachibana for comments. This research was supported in part by RIKEN BNL Research Center and the U.S. Department of Energy under cooperative research agreement #DE-AC02-98CH10886.

* Electronic address: fuku@quark.phy.bnl.gov
† Electronic address: warringa@quark.phy.bnl.gov

[1] For reviews, see; K. Rajagopal and F. Wilczek, arXiv:hep-ph/0011333; M. Alford and K. Rajagopal, arXiv:hep-ph/0606157.
[2] S. L. Shapiro and S. A. Teukolsky, "*Black holes, while dwarfs, and neutron stars, the physics of compact objects*", (John Wiley & Sons, 1983).
[3] For a recent review, see; J. M. Lattimer and M. Prakash, Phys. Rept. **442**, 109 (2007).
[4] K. Iida and G. Baym, Phys. Rev. D **63**, 074018 (2001). M. Alford and K. Rajagopal, JHEP **0206**, 031 (2002);
[5] R. C. Duncan and C. Thompson, Astrophys. J. **392**, L9 (1992).
[6] D. Lai and S. L. Shapiro, Astrophys. J. **383**, 745 (1991).
[7] V. P. Gusynin, V. A. Miransky and I. A. Shovkovy, Phys. Rev. Lett. **73**, 3499 (1994); Phys. Rev. D **52**, 4718 (1995).

[8] D. Ebert, K. G. Klimenko, M. A. Vdovichenko and A. S. Vshivtsev, Phys. Rev. D **61**, 025005 (2000).
[9] M. G. Alford, J. Berges and K. Rajagopal, Nucl. Phys. B **571**, 269 (2000).
[10] E. J. Ferrer, V. de la Incera and C. Manuel, Phys. Rev. Lett. **95**, 152002 (2005); Nucl. Phys. B **747**, 88 (2006).
[11] C. Manuel, PoS **JHW2005**, 011 (2006).
[12] E. J. Ferrer and V. de la Incera, arXiv:nucl-th/0703034.
[13] M. Buballa, Phys. Rept. **407**, 205 (2005).
[14] E. V. Gorbar, Phys. Rev. D **62**, 014007 (2000).
[15] K. Fukushima and H. J. Warringa, in preparation.
[16] K. Fukushima, C. Kouvaris and K. Rajagopal, Phys. Rev. D **71**, 034002 (2005); S. B. Ruester, I. A. Shovkovy and D. H. Rischke, Nucl. Phys. A **743**, 127 (2004).
[17] H. J. Warringa, D. Boer and J. O. Andersen, Phys. Rev. D **72**, 014015 (2005).
[18] K. Rajagopal and F. Wilczek, Phys. Rev. Lett. **86**, 3492 (2001).